International Journal of Heat and Mass Transfer 147 (2020) 118911

Contents lists available at ScienceDirect

International Journal of Heat and Mass Transfer

journal homepage: www.elsevier.com/locate/ijhmt

Naturally cooled heat sinks for battery chargers

Zhongchen Zhang [a], Eric Lau [b], Chris Botting [b], Majid Bahrami [a,*]

[a] Laboratory for Alternative Energy Conversion (LAEC), School of Mechatronic Systems Engineering, Simon Fraser University, 250-13450, 102 Avenue, Surrey, BC V3T 0A3, Canada
[b] Delta-Q Technologies, 3755 Willingdon Ave, Burnaby, BC V5G 3H3, Canada

ARTICLE INFO

Article history:
Received 25 July 2019
Received in revised form 8 October 2019
Accepted 15 October 2019

Keywords:
Natural convection
Thermal radiation
Fin geometries
Anodization
Battery chargers
Power electronics

ABSTRACT

The objective of this study is to significantly enhance the heat removal capacity of naturally cooled heat sinks (NCHx) of battery chargers for small electric vehicles. To this end, thermal performance of NCHx with various fin geometries and identical footprints, are experimentally and numerically studied under multiple orientations, namely: (i) horizontal, (ii) vertical, and (iii) sideways. The effect of surface anodization is also investigated. A number of finned heat sinks are designed and prototyped including (i) inclined fins (benchmark case), (ii) inclined interrupted fins, (iii) straight interrupted fins, and (iv) pin fins. Studied NCHx share the same footprint of a commercial battery charger IC650 from Delta-Q Technologies. The experimental results before the surface anodization indicate that the inclined interrupted fins can offer the desired thermal improvement under all tested orientations compared to the benchmark case, while the straight interrupted fins are more suitable for applications at vertical orientation and the pin fins operate relatively better at horizontal orientation. A notable overall enhancement of thermal performance, up to 27%, is achieved after anodization, depending on the fin geometries and orientations. The study also shows that the inclined interrupted fin heat sink is the most versatile to operate under various installation orientations, where it can improve thermal performance up to 21%, 24%, and 22%, at horizontal, vertical, and sideways orientation respectively, due to enhancements in both natural convection and thermal radiation.

1. Introduction

Naturally cooled heat sinks (NCHx) have always been used as a preferred method for heat removal in power electronics devices due to the absence of external mechanical parts, e.g. fans and pumps. They offer several advantages including noise-free operation, zero-parasitic energy consumption and high reliability which are desirable in the application of harsh environments such as automotive, military and oil exploration industries [1,2]. Regardless of all the advantages, the comparatively low heat transfer coefficient, usually between 2 and 25 $W{\cdot}m^{-2}{\cdot}k^{-1}$ [3], limits their board applications. Total heat dissipation from a naturally cooled heat sink occurs via natural convection and thermal radiation where fin geometries and surface finishing are the two major dominating factors controlling the heat transfer in NCHx. Poor selected and/or inappropriate fin design can impede the buoyancy-driven airflow which profoundly impacts the convective heat transfer. The objective of this study is to assess potential thermal performance improvements in NCHx operating at various orientations. To achieve this goal, we examine a number of novel fin geometries developed for a battery charger, IC650, from Delta-Q Technologies [Fig. 1]. In the literature, natural convection from finned heat sinks has been explored analytically, numerically, and experimentally. The following summarizes the pertinent studies for straight continuous, inclined, interrupted, and pin fins that have been used to benchmark the present study.

Straight fins: Natural convection from continuous straight finned heat sink are well-developed subjects in the literature. The pioneering studies and efforts include [4–8] and they present several analytical and experimental approaches to investigate the heat transfer behaviors. Bar-Cohen and Rohsenow [9] performed a semi-analytical study for isothermal vertical placed parallel plates and developed a relationship for optimal fin spacing:

$$Nu_s = \left[\frac{576}{\left(\frac{Ra_S S}{L}\right)^2} + \frac{2.873}{\left(\frac{Ra_S S}{L}\right)^{0.5}}\right]^{0.5} \quad (1)$$

This correlation has been validated by several independent studies and widely used in determining the optimal spacing for parallel fins in NCHx. Horizontally-placed straight finned arrays have also been studied [10–12]. Starner and McManus [13] per-

* Corresponding author.
E-mail address: mbahrami@sfu.ca (M. Bahrami).

https://doi.org/10.1016/j.ijheatmasstransfer.2019.118911
0017-9310/

Nomenclature

A	surface area [m^2]
c_p	specific heat [$J{\cdot}kg^{-1}{\cdot}K^{-1}$]
D	pin diameter [m]
F	view factor
g	gravity acceleration [$m{\cdot}s^{-2}$]
G	fin gap distance [m]
Gr	Grashof number
h	heat transfer coefficient [$W{\cdot}m^{-2}{\cdot}K^{-1}$]
H	height [m]
I	column interval distance [m]
I_0	current (A)
k	thermal conductivity [$W{\cdot}m^{-1}{\cdot}K^{-1}$]
L	length [m]
n	number of fins in each column
N	Number of fin columns
Nu	Nusselt number
P	pressure [Pa]
Pr	Prandtl number
q	heat flux [$W{\cdot}m^{-2}$]
Q	heat generation rate [W]
r	surface distance [m]
Ra	Rayleigh number
s	standard deviation
S	fin spacing [m]
t	fin thickness [m]/time [s]
T	temperature [K]
u	velocity [$m{\cdot}s^{-1}$]
U	voltage [V]
W	width [m]

Greek symbols

α	thermal diffusivity [$m^2{\cdot}s^{-1}$]
β	thermal expansion coefficient [$1{\cdot}K^{-1}$]
γ	surface thermal reflectivity
δ	uncertainty
Δ	difference
ε	surface thermal emissivity
η	surface visibility
θ	inclination angle [degree]
ν	kinematic Viscosity [$m^2{\cdot}s^{-1}$]
ρ	density [$kg{\cdot}m^{-3}$]
σ	Stefan-Boltzmann constant [$5.67 \times 10^{-8}\ W{\cdot}m^{-2}{\cdot}K^{-4}$]
φ	surface relative angle [degree]

Subscripts

a,∞	ambient properties
ave	average properties
b	fin bottom
base	heat sink base properties
c	chamber ambient properties
fin	heat sink fin properties
h	horizontal direction
heatsink	heat sink properties
H	fin height as characteristic length scale
L	heat sink length as characteristic length scale
out	heat flux leaving the surface
s	standard deviation
S	fin spacing as characteristic length scale
t	fin top
v	vertical direction
w	wall properties

Abbreviations

CNC	Computer Numerical Control
DAQ	Data Acquisition System
FTIR	Fourier Transform Infrared Reflectometer
NCHx	Naturally Cooled Heat Sinks
PRESTO	Pressure Staggering Option
S2S	Surface to Surface Radiation Model
URF	Under-Relaxation Factor

Fig. 1. IC650 battery charger from Delta-Q technologies.

formed a study on the finned heat sink with three different orientations, vertical, horizontal and 45° inclination. They found that the heat transfer coefficient is 10% to 30% below those of similar vertical fin arrays. Leung and Probert [14] studied the effect of orientations on thermal performance and found out that vertically-placed rectangular finned heat sink always yielded the best results. Shen et al. [15] examined the heat transfer from rectangular fin heat sinks experimentally and numerically, with up to eight inclination angles and reported that the thermal performance for 45°, 135°, 225°, and 315° were almost the same. Tari and Mehrtash [16] also investigated the effect of inclination in a naturally cooled rectangular finned heat sink and proposed a set of correlations for inclined heat sinks.

Inclined fins: Ozoe et al. [17–19] are the pioneering studies of natural convection from a vertically-installed inclined channel. They concluded that the maximum heat transfer rate occurs when the inclination angle was around 50° from a series of experimental and numerical studies. Azevedo and Sparrow [20] investigated an open-ended inclined channel experimentally. Their flow visualization results revealed that the longitudinal vortices along the inclined channel helped improving thermal performance when heated from below. Gupta and Nayak [21] took the idea of inclination to the slot-ventilator, where the maximum heat and mass transfer occurred at 45° for most cases. Varol et al. [22] focused on the case when a corner heater existed in an inclined enclosure and the maximum heat transfer happened when the enclosure was inclined at 135°, where inclination angle of 60° yielded the minimum heat dissipation rate. Additional studies can be found in [23–26] that focused on inclined channels with various heat source displacement and cooling medium. However, there is not enough literature to support the natural convection from a heat sink comprised of inclined fins. To the best of our knowledge, Fujii [27] is

one of the studies focused on this particular heat sink geometry. He performed a sequence of experimental studies and concluded that 19% improvement could be gained from 60° inclined fins when compared to 90° straight fins. His experimental result was validated to the following presented correlation:

$$Gr_s = \frac{g\beta S^3 (T_w - T_a)}{\upsilon^2} \cdot \cos\left(\frac{\pi}{2} - \theta\right) \tag{2}$$

$$Nu_s = \frac{1}{24}(Gr_S Pr)\left(\frac{S}{W_{fin}}\right)\left[1 - e^{\frac{-12.5}{\left(\frac{Gr_S Pr S}{W_{fin}}\right)^{\frac{3}{4}}}}\right] \tag{3}$$

This empirical model should be further validated and suggested for the future studies in inclined finned heat sinks.

Interrupted fins: Effect of fin interruptions on NCHx is a well-established topic in the literature. The idea with interrupted fins is forcing the entrance region of the thermal boundary layer where maximum heat transfer happens, to reset and rebuild. Studies including [28–31] represent some of the efforts to examine and implement the idea of interruption to enhance the natural convection. Gorobets [32] numerically calculated that heat transfer was intensified by 50–70% for a vertical surface with discrete fins arrangement. Ahmadi et al. [33] developed a novel analytical model using the integral technique on interrupted fins where they performed a series of studies to investigate the effect of interruption in straight continuous fins at the vertical orientation. A heat sink design procedure has been suggested to find the best fin arrangement to maximize the total heat transfer from such finned heat sinks. They reported that an optimum fin spacing for interrupted fins remains unchanged as compared with continuous fins and it can be calculated by the correlation as Eq. (1) provided by [9]. However, they only focused on the case where the heat sink was tested in the vertical orientation. Additional efforts are required for investigating the orientational effect in this particular heat sink fin geometry. More studies, including [34–36], further confirmed the prominent impact of fin interruption where interrupted fins can be an effective and efficient design for NCHx.

Pin fins: The alternation of traditional fins into either circular or square rods can also be a potential method to reduce the thermal resistance in NCHx. Most of the existing studies are done by either experimental or numerical approaches. The alignment of the pins can be classified into two categories, staggered or in-line, as shown in Fig. 2. Aihara et al. [37] performed an experimental study on staggered pin fins with a vertical base and proposed an optimal range for the ratio of vertical pin spacing to the diameter, S_v/D = 1–4 when $Gr_H = 10^6$–10^8. Zografos and Sunderland [38] concluded that the in-line arrangement of pins yielded up to 20% better performance compared to the staggered arrangement for vertical orientations under natural convection. They also discussed the effect of heat sink inclination (60°–90°) where no significant difference was observed. Fisher and Sahray et al. [39] used both numerical and experimental methods to optimize the in-line square pin fin arrays in a horizontal orientation and to conclude that an optimal pin density existed with pin spacing to width ratio approximately of 3. The optimization studies of pin fins for natural convection have also conducted with the following efforts [40–42].

In spite of the above-mentioned fin geometries, additional studies for trapezoidal [43] and exponential fins [44] also reveal promising improvement in heat dissipation rate and fin efficiency. Nevertheless, it remains challenging to implement those results in real product designs because most of the investigations have been conducted with diverse heat sink footprints, i.e., base area, volume, and height. Furthermore, the vast majority of the studies regarding natural convection only focused on the vertical orientations where it is explicitly implied by the direction of gravity acceleration where the thermal and hydraulic resistance can be minimized. In this work, four heat sinks are designed and prototyped bearing the same footprint as a commercial power electronic products, battery charger IC650 from Delta-Q Technologies, with various fin geometries, i.e., (i) inclined fins, (ii) inclined interrupted fins, (iii) straight interrupted fins, and (iv) pin fins, to investigate their thermal performance at various orientations. All heat sinks are tested at three orientations including (i) horizontal, (ii) vertical, and (iii) sideways, before and after surface anodization to also quantify its impact of radiation heat transfer on NCHx. A custom-built natural convection and thermal radiation test chamber has been designed to conduct the thermal tests. A numerical model is developed in Ansys Fluent 17.2 and validated to decouple the amount of thermal radiation from the overall heat transfer.

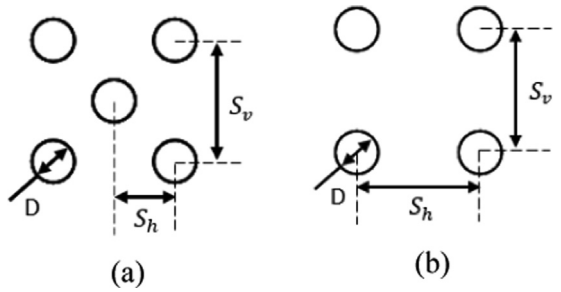

Fig. 2. Pin fin alignment: (a) staggered; (b) in-line.

2. Sample preparations

2.1. Heat sink prototyping

All heat sinks were prototyped using Computer Numerical Control (CNC) machining tool in-house in our School with aluminum alloy 6061-T6 [thermal conductivity $k = 150\ \mathrm{W{\cdot}m^{-1}{\cdot}K^{-1}}$]. The anodization was done by a local surface finishing vendor, "Spectral Finishing, Inc". Type II-Black anodization, the most commonly adopted in commercial products, was chosen and implemented in our prototyped heat sinks to investigate the thermal improvement by radiation. The emissivity measurement has been done using Fourier Transform Infrared Reflectometer (FTIR) and the measured emissivity value for the anodized surface was 0.89. The measurement details can be found in [45]. The heat sink base dimension was 18 cm × 16 cm and the base thickness was 0.35 cm. The fin height in all samples was 6 cm. A draft angle of 1.5° for inclined fins was used as their current design in the products and 1° for rest of heat sinks' fins, to resemble the potential improvement in aluminum die-cast manufacturing technologies available on the market. Fig. 3 shows all prototyped heat sinks with schematics of the top view. The detailed consideration and dimensions for each heat sinks are discussed in the following section.

2.2. Geometrical details

The inclined finned heat sink design was provided by Delta-Q Technologies and served as the benchmark case to illustrate the potential improvement by varying the fin geometry. The inclined interrupted fins simply took the idea of interruption where the long inclined fins have been sectioned into shorter fins to interrupt and reset the thermal and the hydrodynamic boundary layers so as to increase the overall heat transfer rate. In the inclined interrupted fin design, eight columns of relative short fins replaced the initial four columns of long fins with varying lengths. The number of fins in each column were kept the same [$n = 12$]. The fin

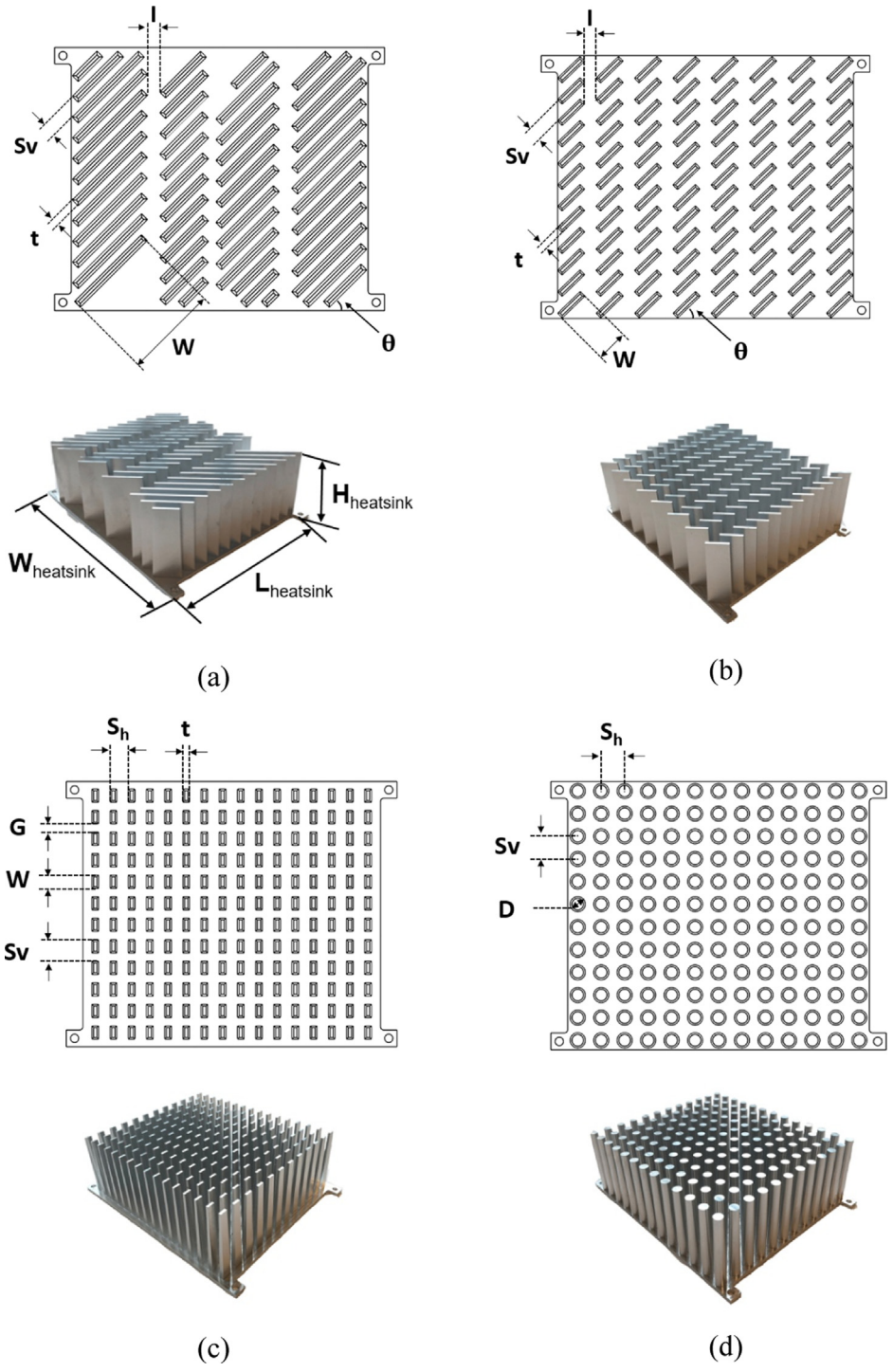

Fig. 3. Prototyped heat sinks with schematic of top view: (a) inclined fins; (b) inclined interrupted fins; (c) straight interrupted fins; (d) pin fins.

spacing of the inclined interrupted design was slightly expanded due to the reduction of the draft angle from 1.5° to 1°. The rest of the geometrical dimensions were maintained as the same as in the benchmark heat sink.

The proposed straight interrupted fin design was based on the studies by Ahmadi et al. [33,36]. The selection of gap distance is usually from considerations such as manufacturing, cost, and weight because the increase of gap length (G) has an adverse effect on the overall thermal performance as shown in their studies. Thus we selected 0.5 cm for gap distance as the minimum fin to fin spacing that can be achieved by current die-cast technologies indicated in [46]. The width of the fin was set to 0.8 cm based on the optimal ratio of the fin width to the heat sink length which is approximately 0.05 as suggested by their parametrical results.

In our particular pin fins design, the top pin diameter was preset as 0.69 cm as the same size of the pin posts on the current die-cast model to mimic the actual castable heat sinks. The pin diameter at the bottom was 0.90 cm because of the draft angles imposed on the fins. Given the size of the pin diameter, limited information can be found to assist the design of the optimal fin spacing in the current literature. Therefore, a numerical investigation on the effect of pin spacing was carried out based on a developed conju-

gate numerical heat transfer model. A detailed description of the numerical model and parametric study can be found in [45]. The results show an optimal fin spacing existed for this particular case has a pin diameter of 0.9 cm at the bottom. The optimal horizontal center to center spacing is approximately 1.4 cm for heat sinks operating at both horizontal and vertical orientations. Table 1 shows the geometrical details of the four prototyped NCHx. More details regarding the selection of the range of the parameters are available in [45] where industry practice and manufacturing limitations can play a major part.

The geometrical data from Table 1 also shows the variation of weight and surface area variation between proposed heat sinks. Inclined and straight interrupted fins have reduced weight and surface area significantly because of the idea in fin interruption, the replacement of long fins with shorter fins. The reduction in weight potentially implies a decrease in manufacturing material cost but other factors such as tooling cost are equally important. On the other hand, the mechanical strength of the fins can be minimized due to the small fin dimensions to resist external forces. The weight of the pin fin heat sink is increased compared with the benchmark case attributed to the comparatively larger pin diameter, up to 0.9 cm, which also suggests the durability and high mechanical strength of the pins.

3. Experimental study

A custom-designed testbed was developed to perform steady-state thermal tests. As an effort to reduce the air-flow disturbance and provide a uniform radiation background, a specified test chamber [0.5 m × 0.5 m × 0.5 m] was built with 4 mm thick acrylic plastics. The surface emissivity of acrylic plastic was approximately 0.9 in the range of wavelength in infrared spectrum with physical and thermal properties of density [ρ = 1180 kg·m^{-3}], thermal conductivity [k = 0.2 W·m^{-1}·K^{-1}], and specific heat [c_p = 1470 J·kg^{-1}·K^{-1}]. The tested heat sinks were mounted on an insulating substrate with a structure of wooden plate [1 cm], polyester foam [2 cm], and wooden plate [1 cm]. An electrically-insulated Kapton heater, size of 10 cm × 15 cm, was installed at the back of the heat sink providing thermal power to the system with a layer of high thermally conductive paste [OMEGATHERM 201] at the interface to minimize the thermal contact resistance between the heater and baseplate. A programmable DC power supply [Chroma 62012P-100-50] was used to provide electrical power. T-type [copper-constantan] thermocouples were used to monitor the temperature distribution along the enclosure base, chamber ambient, and chamber walls. A NI-9212 [National Instrument] temperature acquisition module and a NI-9229 [National Instrument] voltage analog input unit were connected to a compact DAQ [cDAQ-9174] chassis to log the data into a PC. The experimental setup is shown in Figs. 4 and 5.

All measurements were carried out in an open lab environment. Each heat sink was tested with input power ranging from 20 W to 100 W at all three orientations, i.e., horizontal, vertical, and sideways. The ambient temperature in the lab was maintained at 22 °C. Thermal tests of each heat sink were repeated at least three times with a steady-state criterion of ∂T/∂t less than 0.001 for 30 min. Each prototyped heat sink was tested in the same manner before and after the anodization. Fig. 6 shows the schematic of the test heat sinks placed at three orientations.

3.1. Uncertainty analysis

Voltage (U), current (I_0), and temperature (T) are the three measured parameters in this experiment. According to the equipment specification from National Instrument, the voltage acquisition modules has a maximum error of ±1.2% when it has not been calibrated. The T-type thermocouples we used for monitoring the temperature distribution have a maximum uncertainty of ±1 °C. The maximum measurement uncertainty value for the heat generation rate, the temperature difference, and the heat transfer coefficient can be calculated through Eqs. (4)–(7). Because each thermal test was repeated at least three times, the reported maximum uncertainty also includes the standard deviation for each test with the same level of heat input.

$$\frac{\delta \dot{Q}}{\dot{Q}} = \left[\left(\frac{\delta U}{U} \right)^2 + \left(\frac{\delta I_0}{I_0} \right)^2 \right]^{\frac{1}{2}} \tag{4}$$

$$\delta \Delta T = \left[(\delta T)^2 + (\delta T)^2 \right]^{\frac{1}{2}} \tag{5}$$

$$\delta \Delta T_s = \left[(\delta \Delta T)^2 + s_{\Delta T}{}^2 \right]^{\frac{1}{2}} \tag{6}$$

$$\frac{\delta h}{h} = \left[\left(\frac{\delta U}{U} \right)^2 + \left(\frac{\delta I_0}{I_0} \right)^2 + \left(\frac{\delta \Delta T_s}{\Delta T_s} \right)^2 + \left(\frac{\delta L_{heatsink}}{L_{heatsink}} \right)^2 + \left(\frac{\delta W_{heatsink}}{W_{heatsink}} \right)^2 \right]^{\frac{1}{2}} \tag{7}$$

The calculated uncertainty for the input power is ±1.7% and the estimated uncertainty for temperature measurements is ±1.4 °C. For the heat transfer coefficient, the maximum uncertainty is calculated as ±9%. For the calculation of Nusselt (Nu) and Rayleigh (Ra), the characteristic length is not included in the uncertainty analysis since it is not measured and the thermophysical properties including thermal conductivity and expansion coefficient of air which are assumed to be constant. The amount of maximum errors for Nusselt number and Rayleigh number, which is calculated to be 9% and 12%.

Table 1
Comparison of geometrical dimensions for studied heat sinks.

Geometrical parameters	Inclined Fins (Benchmark)	Inclined Interrupted Fins	Straight Interrupted Fins	Pin Fins
Fin vertical spacing (S_v) [cm]	0.89	0.95	1.30	1.37
Horizontal fin spacing (S_h)/Column interval (I) [cm]	0.50/0.80	0.70	1.09	1.42
Fin width (W) [cm]	3.50/6.00	1.90	0.80	–
Fin thickness (t)/diameter (D_t) at fin top [cm]	0.18	0.18	0.18	0.69
Fin thickness (t)/diameter (D_b) at fin bottom [cm]	0.49	0.39	0.39	0.90
Fin inclination angle (θ) [°]	45	44	–	–
Draft angle [°]	1.5	1.0	1.0	1.0
Number of fins in each column [n]	12	12	12	12
Number of fin columns (N)	4	8	16	13
Surface area (A) [m^2]	0.31	0.26	0.25	0.26
Weight [kg]	1.47	1.07	0.92	1.52

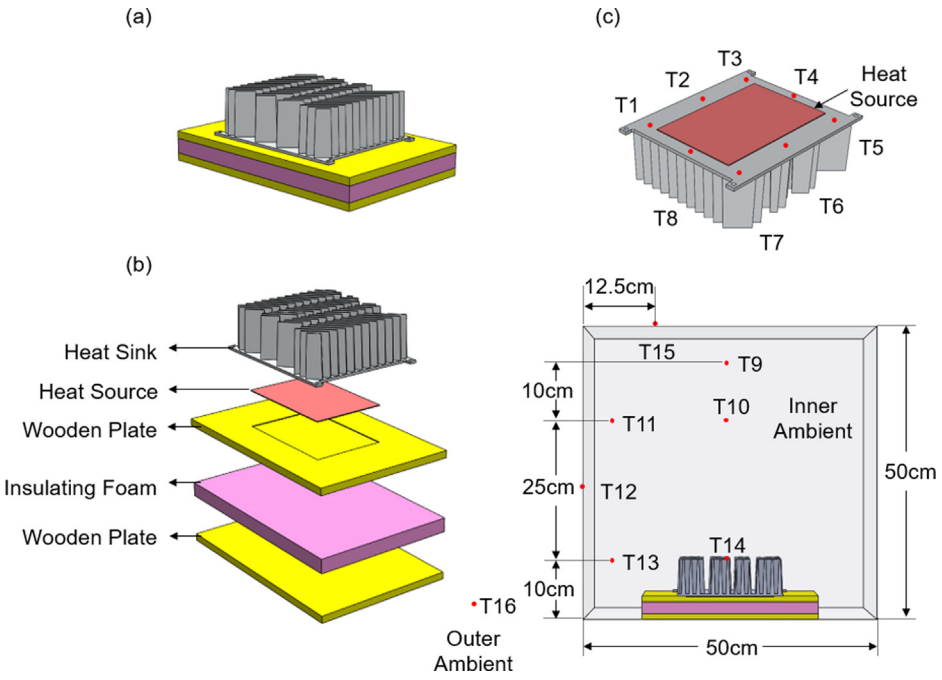

Fig. 4. Schematic of the experimental setup: (a) assembled tested heat sink with insulation substrate; (b) split view of the substrate; (c) location of the installed thermocouples.

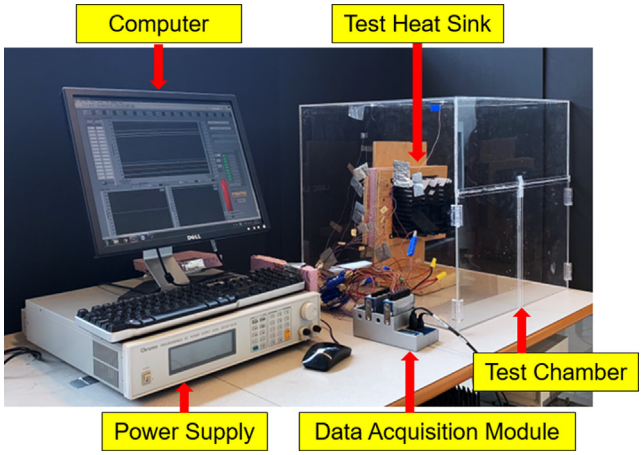

Fig. 5. Custom-built natural convection and thermal radiation experimental setup.

4. Numerical analysis

4.1. Governing equations

A 3-D numerical model was developed for incompressible flow using Ansys Fluent 17.2 to evaluate the heat sink performance and also enable us to decouple the amount of thermal radiation from the overall heat transfer. The flow is assumed to be in steady-state and within the laminar regime, i.e., $Ra < 10^8$. The Boussinesq approximation is imposed for air-density correlation, i.e., the air density is linearly varied with temperature. Since we also consider the thermal radiation, the grey body assumption is valid for the heat sink surfaces and chamber walls where the surface radiative properties, i.e., emissivity and reflectivity, are uniform and independent of the wavelength and the surface temperature. A laminar model for fluid flow and Surface to Surface [S2S] radiation model is used. The governing equations for the fluid are shown from Eqs. (8)–(10) [47]:

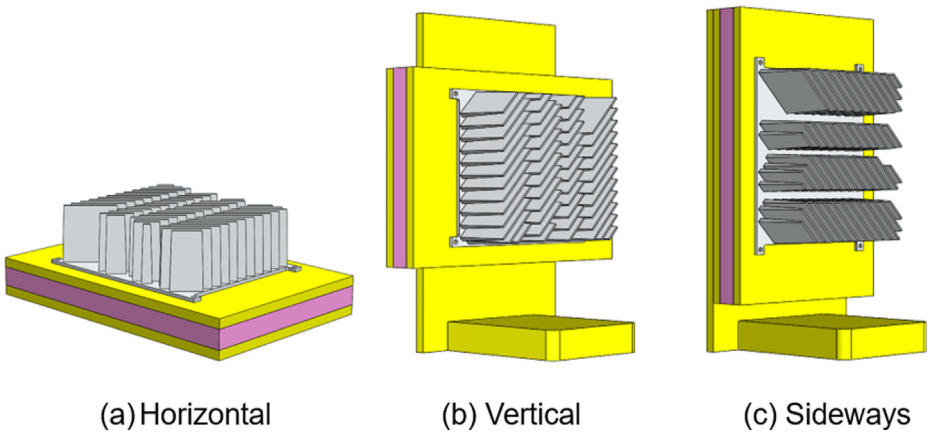

Fig. 6. Test orientations: (a) horizontal; (b) vertical; (c) sideways.

Continuity:

$$\nabla \cdot \vec{u} = 0 \tag{8}$$

Momentum:

$$\vec{u} \cdot \nabla \vec{u} = -\frac{1}{\rho_\infty} \nabla P + \upsilon \nabla^2 \vec{u} - g\beta(T - T_\infty)\hat{n} \tag{9}$$

Energy:

$$\vec{u} \cdot \nabla T = \alpha \nabla^2 T \tag{10}$$

where $\hat{n}$ is the normal vector of the heat sink base and parallel to the gravity acceleration. ρ, μ, and α are the density, the viscosity, and the thermal diffusivity, respectively. The S2S radiation model can be formulated as Eq. (11) neglecting any absorption, emission, and scattering effects in the ambient air where it depicts the radiation heat flux leaving surface i with incident radiation from surface j, for j = 1,2,3,. . .N.

$$q_{out,i} = \varepsilon_i \sigma T_i^4 + \gamma_i \sum_{j=1}^{N} F_{ij} q_{out,j} \tag{11}$$

where F_{ij} is the view factor between surface i and j which indicates the fraction of energy leaving surface j that incidents on surface i. γ is the surface reflectivity and can be calculated as $\gamma = 1 - \varepsilon$ using Kirchhoff's law of radiation. The view factor between the surface i and j is calculated by:

$$F_{ij} = \frac{1}{A_i} \iint_{A_i A_j} \frac{\cos\varphi_i \cos\varphi_j}{\pi r^2} \eta_{ij} dA_i dA_j \tag{12}$$

where A, r are the surface area and the distance. φ are the angle between the direction of radiation and surface normal. η_{ij} is determined by the visibility of dA_i and dA_j and equals to 1 if dA_i is visible to dA_j.

4.2. Boundary conditions

All the walls have no-slip and no-penetration boundary conditions. For the solid-fluid interfaces on the heat sink, the boundary conditions are determined via system coupling. Constant heat flux is assumed at the base of the heat sink as the heat input. The fluid domain walls have a constant temperature with the measured value from the experiments. The surface thermal emissivity for the machined and anodized surface is 0.03 and 0.89 as obtained from our emissivity study [45]. The surface emittance for the ambient walls is 0.9 throughout all simulations.

4.3. Numerical schemes

The momentum and energy terms are discretized by the Power Law scheme and the PRESTO scheme is adopted in the discretization of the pressure term. Because of the high nonlinearity and instability of the natural convection flow, the Under-Relaxation Factor (URF) for momentum is adjusted to 0.35 to dampen the solution and reduce oscillations. The iterations are terminated when the variation of heat sink surface temperature was 1×10^{-4} in the last 100 steps while the residues for continuity, momentum, and energy are converging.

4.4. Mesh independency study

The mesh is constructed with non-conforming tetrahedral and triangular elements with a much finer resolution at the solid-fluid interface, showing in Fig. 7, where the inclined interrupted heat sink model serves as an example. A mesh independence study

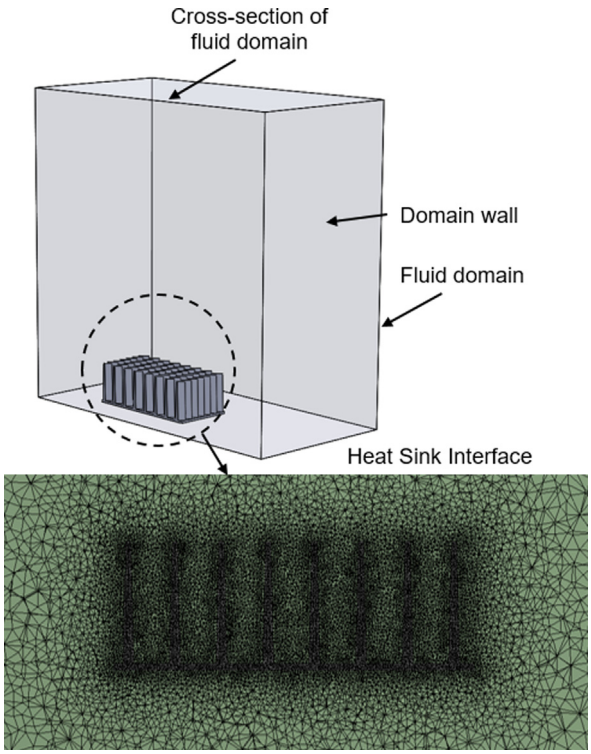

Fig. 7. Mesh distribution, a cross-section of the fluid domain.

was conducted in the case of inclined fins. The result is shown in Fig. 8 and indicates a choice of mesh element number of approximately 6,000,000 leads to a 0.11% deviation from the case with meshing elements of around 8,000,000. Thus, we choose the case where the total element number is around 6,000,000 and the meshing size on the heat sink surface is 1.5×10^{-3} out of the consideration in accuracy and computational cost.

5. Results and discussion

The experimental results for prototyped heat sinks with various fin geometries are presented for both surface conditions, i.e., before and after the surface anodization. Since the measured surface emittance for the machined aluminum surface is 0.03, natural convection contributes to most of the heat transfer occurred on the heat

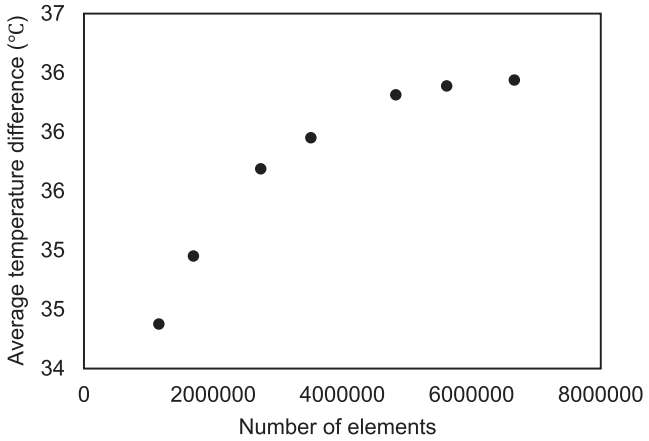

Fig. 8. Mesh independency study, with 80 W thermal input and surface emissivity of 0.89.

sink surfaces. After anodization treatment, the thermal test results are used to validate the numerical model, where the radiative heat transfer can be extrapolated from the numerical simulation results.

5.1. Dimensionless analysis

It is important to formulate the results in terms of the non-dimensional parameters and more informative instruction to the heat sink design can be provided. The characteristic length scale for defining the Nusselt (Nu), Grashof (Gr), and Rayleigh (Ra) number is the length of the prototyped heat sinks [L], shown in Fig. 3. The dimensionless parameter can be calculated through Eqs. (13)–(16).

$$h = \frac{Q}{A\Delta T} \tag{13}$$

$$Nu_L = \frac{hL_{heatsink}}{k} \tag{14}$$

$$Gr_L = \frac{g\beta\Delta T L_{heatsink}{}^3}{\upsilon^2} \tag{15}$$

$$Ra_L = Gr_L Pr \tag{16}$$

where ΔT represents the temperature difference between the average heat sink base and chamber ambient where it is directly measured from the experiments. A is the heat dissipating area for each tested heat sink. k, β are the thermal conductivity and the volumetric expansion coefficient of the air where ν, Pr are the kinematic viscosity and the Prandtl number of the cooling medium, air in this case.

Fig. 9 presents the tested results for untreated heat sinks in the form of the dimensionless parameters where the range of Rayleigh and Nusselt number is indicated. The horizontal error bars represent the maximum uncertainty for Rayleigh number, which is 12%, and the maximal error value for Nusselt number is 9%, shown as vertical error bars. As indicated, for tested heat sinks operating at three different orientations, all calculated Rayleigh numbers are below the 10^8, which suggests the fluid flow for natural convection is within the laminar regime. It is also worth noting that all suggested heat sinks, including the inclined fins design, have their best performance at horizontal orientation while the sideways orientations yield the worst. It is because the spacing between the fins is greatly reduced where less surface area can be in touch with the air-flow and convection heat transfer is greatly minimized when heat sinks are placed vertically and sideways.

5.2. Effect of fin geometries

Fig. 10 shows a comparison between the experimental and numerical results for each prototyped heat sink with the bare surface condition [$\varepsilon = 0.03$] for all three orientations. Temperature difference represents the average heat sink base temperature with

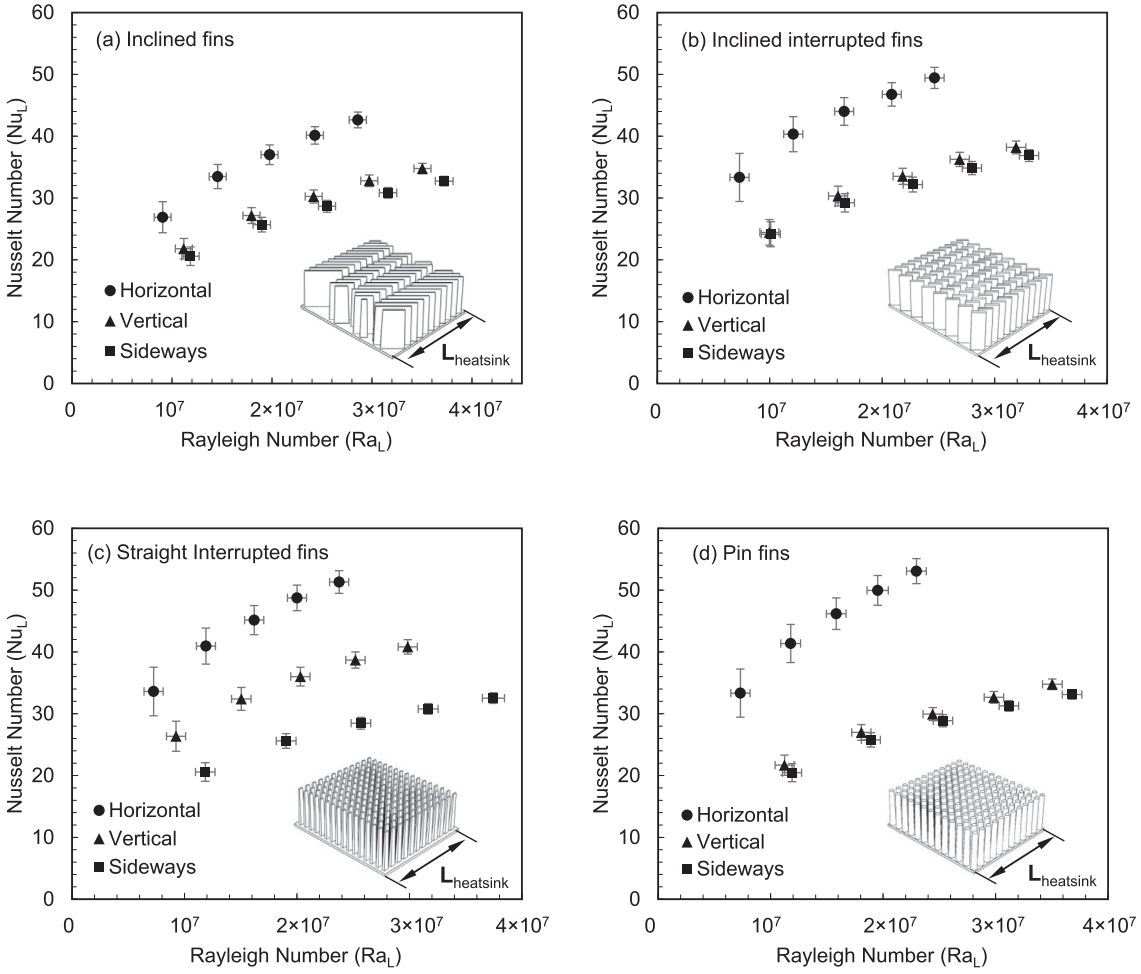

Fig. 9. Dimensionless experimental results of each heat sink with the bare surface condition for three orientations: (a) inclined fins; (b) inclined interrupted fins; (c) straight interrupted fins; (d) pin fins.

reference to the average chamber ambient temperature shown as Eq. (17).

$$\Delta T = T_{base,ave} - T_{c,ave} \tag{17}$$

The symbols indicate the experimental results and the numerical results are presented as solid and dash lines. As shown, the experimental results are in a good arrangement with the present model, with a maximum 5% difference in horizontal orientations, 4% and 12% maximal difference in vertical and sideways orientations, respectively. It should be noted that the heat flux variance showed on the figure is a result of the difference in heat dissipation area where the proposed finned heat sinks have a relatively small area compared to the benchmark design. The following can be concluded from Fig. 10(a): (i) overall thermal performance of all proposed heat sinks have improved compared with the inclined fins design at horizontal orientation; (ii) both straight and inclined interrupted design can also yield a significant improvement, approximately 17% and 14% with a thermal input of 100 W, while the pin fins can provide up to 20% reduction in average base temperature. In terms of thermal performance at the vertical orientation shown in Fig. 10(b), the straight interrupted fin design offers the greatest thermal improvement [15% at 100 W] and inclined interrupted fins are also able to reduce the average base temperature around 5 °C with a heat input of 100 W. On the other hand, the pin fins fail to have any improvement and it may be caused by the relatively larger pin diameter we choose for this special case. As shown in Fig. 10(c) of the heat sinks performance comparison for sideways orientation, only the inclined interrupted design is capable to offer 11% reduction in average base temperature difference where both straight interrupted and pin fins have a restricted contribution to the overall heat transfer due to the geometrical constraints on the airflow. Overall, the thermal impact of fin geometries is prone to the orientation effects where most of the proposed heat sinks can only achieve the desired thermal performance at a specific orientation. However, the inclined interrupted fins design has the versatility to provide a notable amount of thermal enhancement for all three orientations.

5.3. Effect of surface anodization

All of our prototyped heat sinks were also anodized with Type II-Black treatment, which is mostly adopted for cosmetic purposes. The thermal effect of surface anodization is shown in Fig. 11, where it is plotted in contrast to the thermal performance of untreated ones. The horizontal axis denotes the test orientation and the surface condition. The average temperature difference from the heat sink base with respect to the average chamber ambient is chosen as a performance indicator shown as the vertical axis. In all four prototyped heat sinks, a notable improvement can be seen after anodization, depending on the fin geometries and test orientations. With horizontal orientation, the inclined fin design has the most enhancement, approximately 13%, in relative temperature difference, while the performance gain for the rest of the fin geometries is less than 8%. In vertical and sideways orientations, all finned heat sinks show between 10% and 15% thermal improvement. In spite, the thermal performance for vertically and sideways placed heat sinks with proposed fin geometries are greatly improved after the anodization treatment, the average temperature difference is still higher than the case where the heat sinks are placed horizontally. It implies that radiative heat transfer is insufficient to compensate for the weak natural convection performance when heat sinks are operating in a less favorable orientation and substantial resistances are posed to air-flow and heat transfer. The variation of thermal enhancement among different fin geometries and working orientations can also be explained by the fact that thermal radiation is proportional to the surface temperature to the fourth power. Higher surface temperatures will lead to a considerable

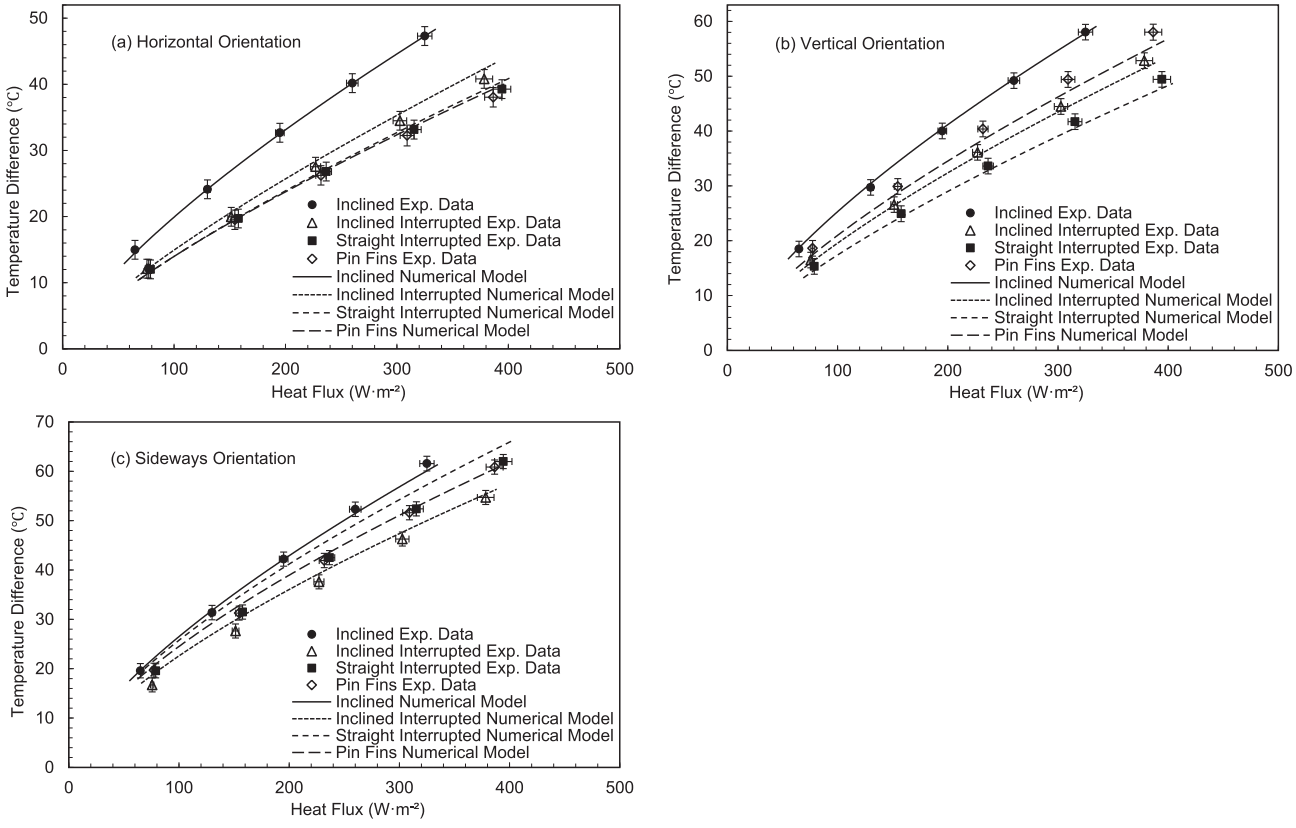

Fig. 10. Comparison of experimental results (symbols) with numerical models (lines) of untreated heat sinks at three orientations: (a) horizontal; (b) vertical; (c) sideways.

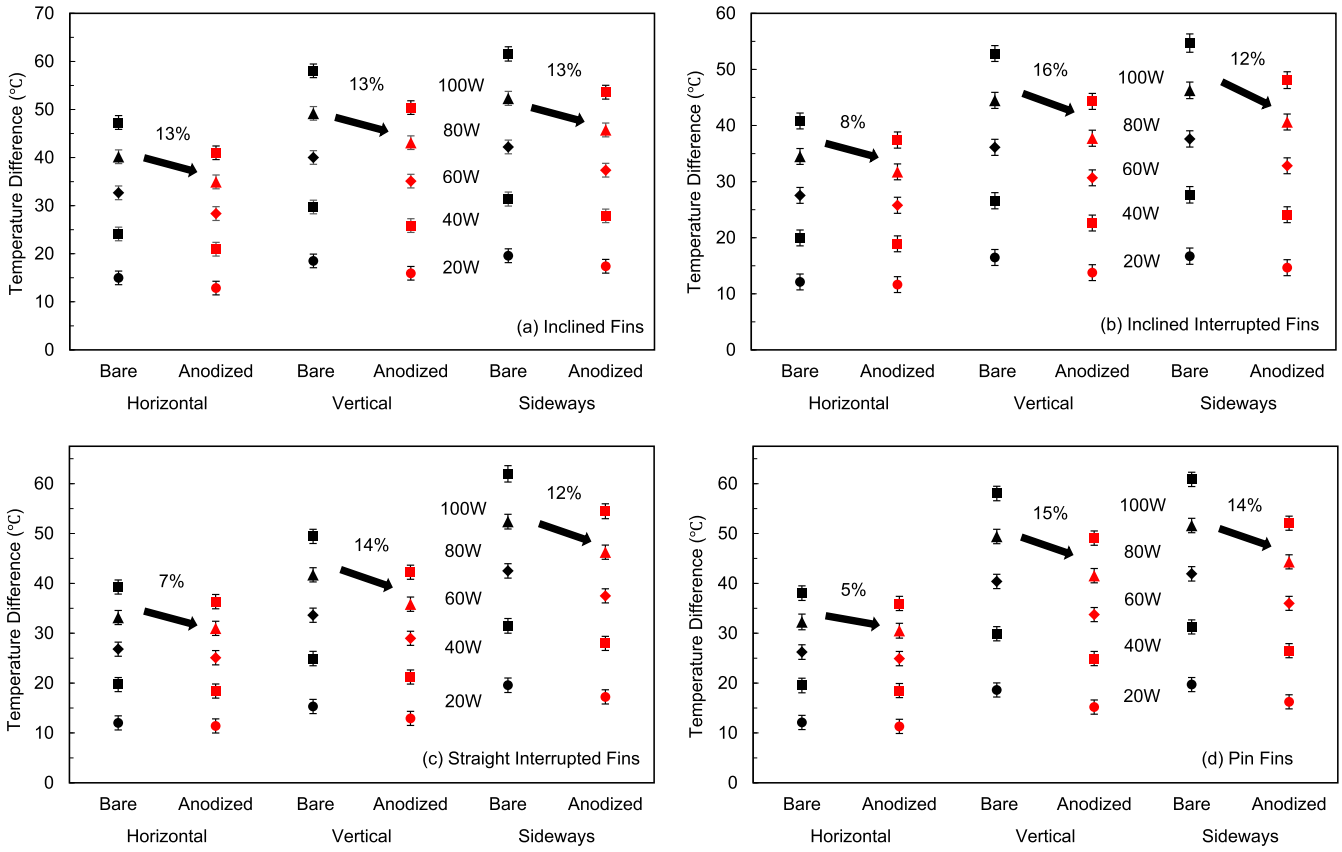

Fig. 11. Comparison of thermal performance of prototyped heat sinks before and after surface anodization for all three orientations: (a) inclined fins; (b) inclined interrupted fins; (c) straight interrupted fins; (d) pin fins.

radiative heat transfer where the overall thermal performance is a combined effect with natural convection of nonlinearly distributed behaviors.

In the meantime, the comparison among each anodized heat sink reveals the identical enhancement to the inclined fins design without surface anodization treatment, as can be seen in Fig. 12. At horizontal orientation, the inclined interrupted fins, straight interrupted fins, and pin fins have thermal improvement of 9%, 11%, and 12%. The relative enhancement is 9% and 15% for inclined and straight interrupted fins where the pin fins have the same performance as the benchmark case at the vertical orientation. At sideways orientation, only the anodized inclined interrupted design can yield around 10% relative improvement to the anodized benchmark (inclined fins) heat sink. This further suggests its versatility to operate at all three orientations.

The validation of the present numerical model is also shown in Fig. 12. As can be seen in Fig. 12(a)–(c), the numerical model predicts the performance of each heat sink, considering both natural convective and radiation heat transfer. The maximum difference of the numerical model from experimental results is 8%, 5%, and 4% for horizontal, vertical, and sideways orientations, respectively, which is within the range of measurement uncertainty. The present numerical model also enables us to calculate the contribution of radiation heat transfer and deconvolute it from the overall heat dissipation to further investigate anodization effect.

Fig. 13 shows the contribution of thermal radiation from each anodized heat sink. The results are computed from the numerical model after it is validated by experimental results. The curves represent the portions of the thermal radiation to the overall heat dissipation. As shown, the significance of radiative heat transfer depends on the fin geometries and working orientations. The contribution of radiative heat transfer varies between 20% and 27% for horizontal orientation while the range can expand to 22–32% and 25–35% for vertical and sideways orientations. This rising trend may be attributed to the relatively high surface temperature and lead by the fact the natural convective heat transfer is minimized when heat sinks are placed in vertical and sideways orientation, as mentioned previously. It is also observed that the relative contribution of the thermal radiation to the convection decreases with respect to the higher thermal input. The explanation lies in the fact that the driving force for the natural convection is greatly improved due to the higher temperature difference as the heat source power increase. The relative significance of thermal radiation can be mitigated despite the absolute amount of radiation is rising. Moreover, the inclined interrupted fins and pin fins possess the same rate of radiation heat transfer while the straight interrupted fins yield the lowest when placed horizontally. At the vertical orientation, the straight interrupted fins still have the lowermost radiation off the surfaces due to the excellent performance in natural convection. However, the inclined interrupted fins have the least amount of radiation at sideways orientation, attributed to the versatility to operate, and showed to have the lowest surface temperature. The inclined fins, the straight interrupted fins, and the pin fins have almost the same contribution of thermal radiation in case of overall heat transfer at sideways orientation.

The proportion of thermal radiation from various finned heat sink varies between 20% and 35% depending on several factors including fin geometries, surface area, test orientations, and surface emissivity. Therefore, the effect of anodization on the overall thermal performance of the above-prototyped heat sink is substantial and should be utilized to improve the overall heat removal capacity of NCHx.

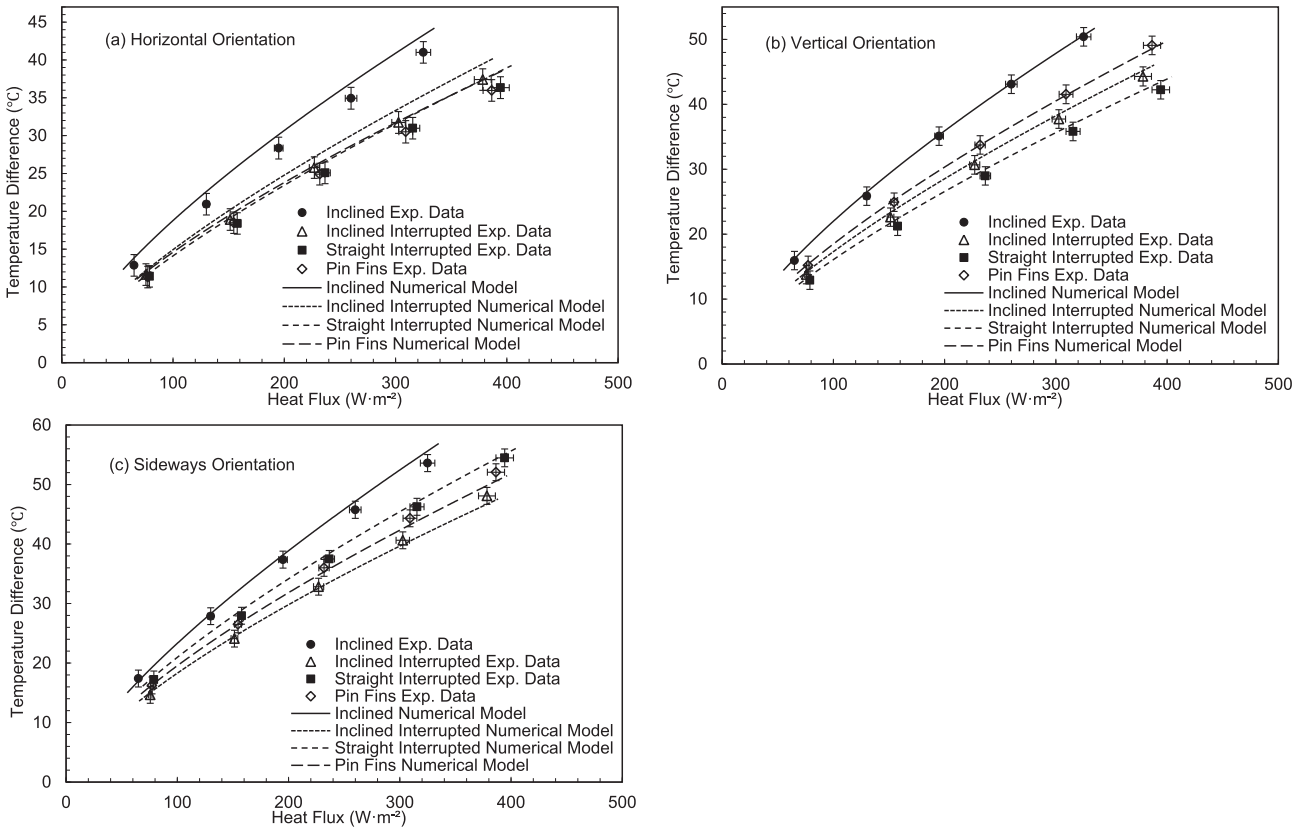

Fig. 12. Comparison of experimental results (solid symbols) with present numerical models (lines) of anodized heat sinks at three orientations: (a) horizontal; (b) vertical; (c) sideways.

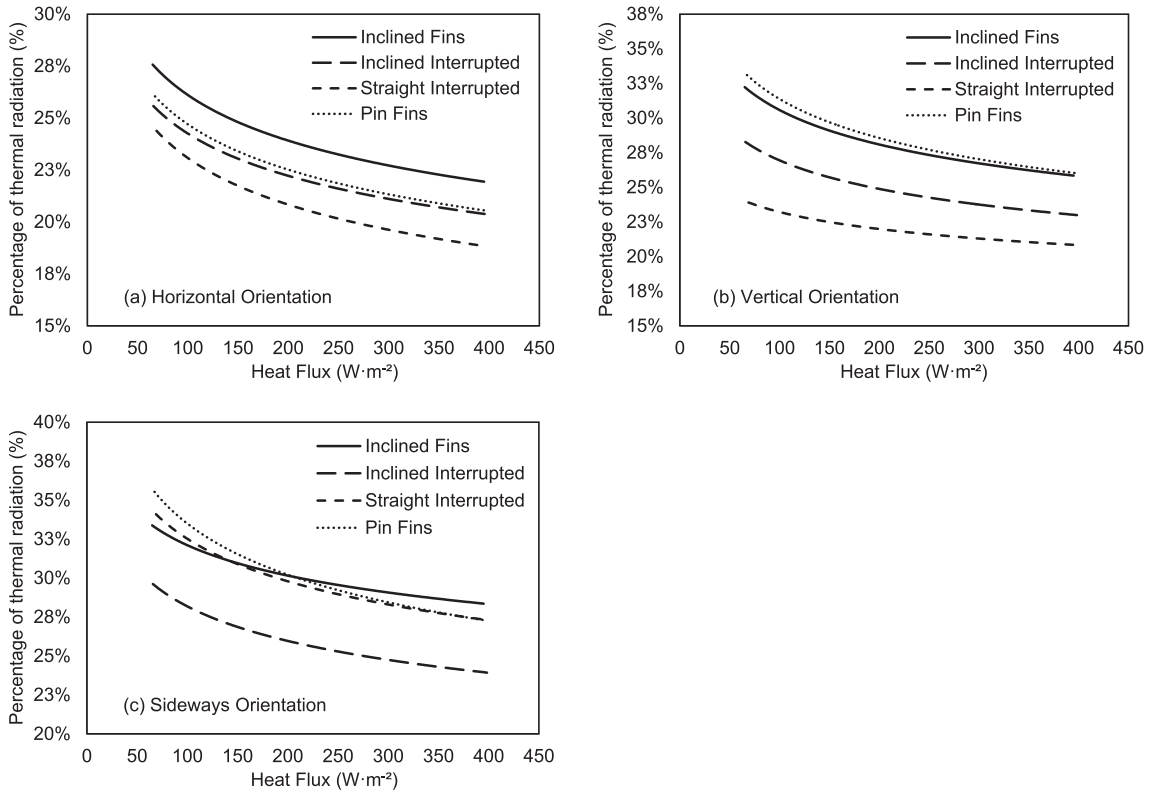

Fig. 13. Contribution of radiation heat transfer in overall heat dissipation from various fin geometries, installed at three orientations, calculated by the present numerical model: (a) horizontal; (b) vertical; (c) sideways.

6. Conclusions

Natural convection and thermal radiation from battery charger heat sinks, with identical footprints and various fin geometries, were investigated through a series of experimental and numerical studies to improve the thermal design of a battery charger. The proposed fin geometries, including inclined interrupted fins, straight interrupted fins, and pin fins, showed a notable thermal improvement in comparison with inclined fins, which resembles the thermal performance of the existing battery charger (IC650) design and served as the benchmark case. After anodization, the overall heat removal capacity of each prototyped heat sink was improved due to the increase in surface thermal emissivity. The major findings of this study can be concluded as:

(1) An enhancement of 20% can be gained by adopting the pin fin design at horizontal orientation. However, the improvement was less prominent for vertical and sideways orientations in case of surface emissivity of 0.03. The bare straight interrupted fins can lead to a 15% reduction in average heat sink base temperature difference for vertical orientation while only 5% was noticed for the sideways orientation. The inclined interrupted design performed the best at sideways orientation where 11% improvement was achieved;
(2) An additional reduction of 5–16% in base temperature difference was observed compared to each untreated heat sink depending on fin geometries and test orientations through anodization treatment. The contribution of thermal radiation ranging from 20% to 35% was observed, where higher surface temperature difference can lead to a higher share;
(3) Considering both the effect of fin geometries and anodization, compared to the inclined fins without surface anodization (benchmark case), the maximal overall improvement, 27%, was gained in vertically placed straight interrupted fins.
(4) The inclined interrupted fins had the versatility to operate at all three orientations where an improvement of 14%, 9%, and 11% was achieved before anodization. In addition, the overall enhancement for inclined interrupted fins after anodizing, the most versatile and promising fin geometry for future applications, was 21%, 24%, and 22%, for each of the orientation respectively.

In terms of future work, more efforts can be put into one of the most promising fin geometries we discovered in this research, the inclined interrupted fins, in the scope of passively cooled systems. Additional efforts can be devoted to developing design protocols in terms of analytical/empirical models and optimization studies. A comprehensive parametric study can be performed to understand the effect of fin spacing and inclination angle on the overall orientational performance for natural convection.

Declaration of Competing Interest

The authors declared that there is no conflict of interest.

Acknowledgment

This research is supported by the funding from the Natural Sciences and Engineering Research Council of Canada (NSERC) Collaborative Research Development (Grant No. CRDPJ488777).

Appendix A. Supplementary material

Supplementary data to this article can be found online at https://doi.org/10.1016/j.ijheatmasstransfer.2019.118911.

References

[1] M. Ohadi, J. Qi, Thermal management of harsh-environment electronics, Annu. IEEE Semicond. Therm. Meas. Manage. Symp. (2004) 231–240, https://doi.org/10.1007/1-4020-3361-3_26.
[2] B. Shang, Y. Ma, R. Hu, C. Yuan, J. Hu, X. Luo, Passive thermal management system for downhole electronics in harsh thermal environments, Appl. Therm. Eng. 118 (2017) 593–599, https://doi.org/10.1016/j.applthermaleng.2017.01.118.
[3] Y.A. Çengel, Introduction to Thermodynamics and Heat Transfer, second ed., Higher Education, McGraw-Hill, New York, 2008, ISBN: 978-0-07-338017-9.
[4] D.W. Van De Pol, J.K. Tierney, Free convection heat transfer from vertical fin-arrays, IEEE Trans. Parts, Hybrids, Packag. 10 (1974) 267–271, https://doi.org/10.1109/TPHP.1974.1134861.
[5] J.R. Welling, C.B. Wooldridge, Free convection heat transfer coefficients from rectangular vertical fins, J. Heat Transfer. 87 (1965) 439, https://doi.org/10.1115/1.3689135.
[6] S.W. Churchill, A comprehensive correlating equation for buoyancy-induced flow in channels, Lett. Heat Mass Transf. 4 (1977) 193–199, https://doi.org/10.1016/0094-4548(77)90132-1.
[7] J.R. Bodoia, J.F. Osterle, The development of free convection between heated vertical plates, J. Heat Transfer. 84 (1962) 40, https://doi.org/10.1115/1.3684288.
[8] E.M. Sparrow, S. Acharya, A natural convection fin with a solution-determined nonmonotonically varying heat transfer coefficient, J. Heat Transfer. 103 (1981) 218, https://doi.org/10.1115/1.3244444.
[9] A. Bar-Cohen, W.M. Rohsenow, Thermally optimum spacing of vertical, natural convection cooled, parallel plates, Trans. ASME. 106 (1984) 116, https://doi.org/10.1115/1.3246622.
[10] F. Harahap, H.N. McManus, Natural convection heat transfer from horizontal rectangular fin arrays, J. Heat Transfer. 89 (1967) 32, https://doi.org/10.1115/1.3614318.
[11] C.D. Jones, L.F. Smith, Optimum arrangement of rectangular fins on horizontal surfaces for free-convection heat transfer, J. Heat Transfer. 92 (1970) 6, https://doi.org/10.1115/1.3449648.
[12] F. Harahap, D. Setio, Correlations for heat dissipation and natural convection heat-transfer from horizontally-based, vertically-finned arrays, Appl. Energy. 69 (2001) 29–38, https://doi.org/10.1016/S0306-2619(00)00073-8.
[13] K.E. Starner, H.N. McManus, An experimental investigation of free-convection heat transfer from rectangular-fin arrays, J. Heat Transfer. 85 (1963) 273, https://doi.org/10.1115/1.3686097.
[14] C.W. Leung, S.D. Probert, Heat-exchanger performance: Effect of orientation, Appl. Energy. 33 (1989) 235–252, https://doi.org/10.1016/0306-2619(89)90057-3.
[15] Q. Shen, D. Sun, Y. Xu, T. Jin, X. Zhao, Orientation effects on natural convection heat dissipation of rectangular fin heat sinks mounted on LEDs, Int. J. Heat Mass Transf. 75 (2014) 462–469, https://doi.org/10.1016/J.IJHEATMASSTRANSFER.2014.03.085.
[16] I. Tari, M. Mehrtash, Natural convection heat transfer from horizontal and slightly inclined plate-fin heat sinks, Appl. Therm. Eng. 61 (2013) 728–736, https://doi.org/10.1016/J.APPLTHERMALENG.2013.09.003.
[17] O. Hiroyuki, S. Hayatoshi, S.W. Churchill, Natural convection in an inclined square channel, Int. J. Heat Mass Transf. 17 (1974) 401–406, https://doi.org/10.1016/0017-9310(74)90011-8.
[18] O. Hiroyuki, Y. Kazumitsu, S. Hayatoshi, S.W. Churchill, Natural circulation in an inclined rectangular channel heated on one side and cooled on the opposing side, Int. J. Heat Mass Transf. 17 (1974) 1209–1217, https://doi.org/10.1016/0017-9310(74)90121-5.
[19] H. Ozoe, H. Sayama, S.W. Churchill, Natural convection in an inclined rectangular channel at various aspect ratios and angles—experimental measurements, Int. J. Heat Mass Transf. 18 (1975) 1425–1431, https://doi.org/10.1016/0017-9310(75)90256-2.
[20] L.F.A. Azevedo, E.M. Sparrow, Natural convection in open-ended inclined channels, J. Heat Transfer. 107 (1985) 893, https://doi.org/10.1115/1.3247518.
[21] N. Gupta, A.K. Nayak, Indoor air performance and irreversibility analysis of a slot-ventilated mechanical system with wall heater and thermosolutal exchanger, Energy Build. 202 (2019), https://doi.org/10.1016/j.enbuild.2019.109344 109344.
[22] Y. Varol, H.F. Oztop, A. Koca, F. Ozgen, Natural convection and fluid flow in inclined enclosure with a corner heater, Appl. Therm. Eng. 29 (2009) 340–350, https://doi.org/10.1016/J.APPLTHERMALENG.2008.02.033.
[23] C.Y. Choi, A. Ortega, Mixed convection in an inclined channel with a discrete heat source, in: [1992 Proceedings] Intersoc. Conf. Therm. Phenom. Electron. Syst., IEEE, n.d.: pp. 40–48. doi: 10.1109/ITHERM.1992.187739.
[24] S. Kiwan, M. Khodier, Natural convection heat transfer in an open-ended inclined channel-partially filled with porous media, Heat Transf. Eng. 29 (2008) 67–75, https://doi.org/10.1080/01457630701677205.
[25] J. Cadafalch, A. Oliva, G. Van Der Graaf, X. Albets, Natural Convection in a Large, Inclined Channel With Asymmetric Heating and Surface Radiation, 2003. doi: 10.1115/1.1571845.
[26] H.X. Yang, Z.J. Zhu, Numerical study on transient laminar natural convection in an inclined parallel- walled channel, Int. Commun. Heat Mass Transf. 30 (2003) 359–367, https://doi.org/10.1016/S0735-1933(03)00054-X.
[27] M. Fujii, Enhancement of natural convection heat transfer from a vertical heated plate using inclined fins, Heat Transf. - Asian Res. 36 (2007) 334–344, https://doi.org/10.1002/htj.20168.

[28] A.K. da Silva, S. Lorente, A. Bejan, Optimal distribution of discrete heat sources on a wall with natural convection, Int. J. Heat Mass Transf. 47 (2004) 203–214, https://doi.org/10.1016/J.IJHEATMASSTRANSFER.2003.07.007.
[29] E.M. Sparrow, C. Prakash, Enhancement of natural convection heat transfer by a staggered array of discrete vertical plates, J. Heat Transfer. 102 (2009) 215, https://doi.org/10.1115/1.3244263.
[30] M.S.S.S. Rao, V.M.K. Sastri, Natural convection heat transfer in staggered vertical channels, Comput. Methods Appl. Mech. Eng. 113 (1994) 263–269, https://doi.org/10.1016/0045-7825(94)90049-3.
[31] N. Gupta, A.K. Nayak, S. Malik, Conjugate heat and species transport in an air filled ventilated enclosure with a thermo-contaminated block, Int. J. Heat Mass Transf. 117 (2018) 388–411, https://doi.org/10.1016/j.ijheatmasstransfer.2017.10.028.
[32] V.G. Gorobets, Heat transfer for vertical surfaces with discrete fins in the case of free convection, J. Eng. Phys. Thermophys. 75 (2002) 1130–1138, https://doi.org/10.1023/A:1021167625009.
[33] M. Ahmadi, M.F. Pakdaman, M. Bahrami, Pushing the limits of vertical naturally-cooled heatsinks; Calculations and design methodology, Int. J. Heat Mass Transf. 87 (2015) 11–23, https://doi.org/10.1016/j.ijheatmasstransfer.2015.03.086.
[34] A. Daloglu, T. Ayhan, Natural convection in a periodically finned vertical channel, Int. Commun. Heat Mass Transf. 26 (1999) 1175–1182, https://doi.org/10.1016/S0735-1933(99)00107-4.
[35] M. Ahmadi, G. Mostafavi, M. Bahrami, Natural convection from interrupted vertical walls, J. Heat Transfer. 136 (2014), https://doi.org/10.1115/1.4028369 112501.
[36] M. Ahmadi, G. Mostafavi, M. Bahrami, Natural convection from rectangular interrupted fins, Int. J. Therm. Sci. 82 (2014) 62–71, https://doi.org/10.1016/J.IJTHERMALSCI.2014.03.016.
[37] T. Aihara, S. Maruyama, S. Kobayakawa, Free convective/radiative heat transfer from pin-fin arrays with a vertical base plate (general representation of heat transfer performance), Int. J. Heat Mass Transf. 33 (1990) 1223–1232, https://doi.org/10.1016/0017-9310(90)90253-Q.
[38] A.I. Zografos, J. Edward Sunderland, Natural convection from pin fin arrays, Exp. Therm. Fluid Sci. 3 (1990) 440–449, https://doi.org/10.1016/0894-1777(90)90042-6.
[39] D. Sahray, H. Shmueli, G. Ziskind, R. Letan, Study and optimization of horizontal-base pin-fin heat sinks in natural convection and radiation, J. Heat Transfer. 132 (2009), https://doi.org/10.1115/1.3156791 012503.
[40] M. Iyengar, A. Bar-Cohen, Least-material optimization of vertical pin-fin, plate-fin, and triangular-fin heat sinks in natural convective heat transfer, in: ITherm'98. Sixth Intersoc. Conf. Therm. Thermomechanical Phenom. Electron. Syst. (Cat. No.98CH36208), IEEE, 2002, pp. 295–302. doi: 10.1109/itherm.1998.689577.
[41] Y. Joo, S.J. Kim, Comparison of thermal performance between plate-fin and pin-fin heat sinks in natural convection, Int. J. Heat Mass Transf. 83 (2015) 345–356, https://doi.org/10.1016/j.ijheatmasstransfer.2014.12.023.
[42] T.S. Fisher, K.E. Torrance, Free convection limits for pin-fin cooling, J. Heat Transfer. 120 (1998) 633, https://doi.org/10.1115/1.2824325.
[43] M. Turkyilmazoglu, Efficiency of the longitudinal fins of trapezoidal profile in motion, J. Heat Transfer. 139 (2017) 3–6, https://doi.org/10.1115/1.4036328.
[44] M. Turkyilmazoglu, Heat transfer from moving exponential fins exposed to heat generation, Int. J. Heat Mass Transf. (2018), https://doi.org/10.1016/j.ijheatmasstransfer.2017.08.091.
[45] Z. Zhang, Passive cooling system: an integrated solution to the applications in power electronics, Simon Fraser University, 2019, (submitted for publication).
[46] A. Sce, L. Caporale, High Density Die Casting (HDDC): New frontiers in the manufacturing of heat sinks, J. Phys. Conf. Ser. 525 (2014), https://doi.org/10.1088/1742-6596/525/1/012020.
[47] P. Wesseling, in: Principles of Computational Fluid Dynamics, Springer Berlin Heidelberg, Berlin, Heidelberg, 2001, https://doi.org/10.1007/978-3-642-05146-3.